

DUAL-TRANSDUCTION ELECTROMECHANICAL RECEIVER FOR NEAR-FIELD WIRELESS POWER TRANSMISSION

Spencer E. Smith, Miah A. Halim, Adrian A. Rendon-Hernandez, and David P. Arnold
Interdisciplinary Microsystems Group, University of Florida, Gainesville FL, USA

ABSTRACT

We report the design, fabrication, and experimental characterization of a chip-sized electromechanical micro-receiver for low-frequency, near-field wireless power transmission that employs both electrodynamic and piezoelectric transductions to achieve a high power density and high output voltage while maintaining a low profile. The 0.09 cm^3 device comprises a laser-machined titanium suspension, one NdFeB magnet, two PZT-5A piezo-ceramic patches, and a precision-manufactured micro-coil with a thickness of only 1.65 mm. The device generates $520 \mu\text{W}$ average power ($5.5 \text{ mW}\cdot\text{cm}^{-3}$) at 4 cm distance from a transmitter coil operating at 734.6 Hz and within safe human exposure limits. Compared to a previously reported piezoelectric-only prototype, this device generates $\sim 2.5\times$ higher power and offers 18% increased normalized power density ($6.5 \text{ mW}\cdot\text{cm}^{-3}\cdot\text{mT}^{-2}$) for potential improvement in wirelessly charging wearables and bio-implants.

KEYWORDS

Electrodynamic, electromechanical coupling, piezoelectric, torsional resonance, wireless power transmission.

INTRODUCTION

As electronic devices become smaller and more portable, wireless power transmission (WPT) has become increasingly popular for device recharging [1,2]. A growing sub-field in WPT is electrodynamic wireless power transmission (EWPT), which involves a mechanically resonating permanent magnet within a receiver. The mechanical energy of the resonating magnet is converted into electricity using one or more electromechanical transduction schemes (e.g. electromagnetic, piezoelectric, or capacitive) [3]. Compared to other WPT schemes, EWPT leverages low-frequency magnetic fields ($<1 \text{ kHz}$), which safely pass through conductive media and have higher human field exposure limits ($\sim 2 \text{ mT}_{\text{rms}}$ at 1 kHz) [4].

Within an EWPT receiver, the most commonly explored electromechanical transduction schemes are electrodynamic (ED) and piezoelectric (PE). ED (sometimes called ‘electromagnetic’) schemes use the motion of the resonating magnet to generate an induced voltage in a receiver coil. Alternatively, PE methods use the resonating magnet to generate stress and consequently voltage in piezoelectric materials integrated within the receiver system. As is well known to the electromechanical transducers and energy-harvesting community, ED transducers generally produce lower voltage and higher currents, whereas PE transducers produce higher voltages and lower currents; or, equivalently, ED transducers have lower output impedance than PE transducers. For example, in [5], for a magnetic field strength of $\sim 0.4 \text{ mT}_{\text{rms}}$, the induced voltage

for the reported ED EWPT receiver was relatively low ($\sim 2.1 \text{ V}_{\text{rms}}$), but a few milliwatts of power ($\sim 1.8 \text{ mW}$) were generated. Under similar conditions, a PE device generated much higher voltages ($\sim 9.2 \text{ V}_{\text{rms}}$) but produced a lower average power ($\sim 0.13 \text{ mW}$) [6]. Higher output voltages are generally desired to enable higher power efficiency in the power management electronics that are required to convert the ac power waveforms into stable dc waveforms for charging batteries or powering devices such as sensors or electronic circuits. Another difference between ED and PE transducers is the overall size (and thickness) of the receiver. Because of the need for multi-turn coils, ED transducers tend to have a bulkier volume and thicker profile than PE transducers. For the previously reported designs, the ED transducer had a thickness of 4.7 mm [5], whereas the PE transducer was only 1.5 mm [6]. For integration with other modern electronics, a low profile is a critical requirement.

With these tradeoffs in mind, this paper explores the use of a combination of ED and PE transduction within an EWPT receiver, which is sometimes used in kinetic energy harvesting [7]. In this case, the design objective is to simultaneously generate higher voltages than a pure ED transducer [5] and higher time-average power than a pure PE transducer [6], while maintaining a low profile. Herein, we report the design, fabrication, and testing of a chip-sized EWPT receiver with an innovative, volume-efficient architecture intended to meet these goals.

RECEIVER DESIGN AND OPERATION

Figure 1 presents the schematic of the dual-transduction mode micro-receiver. The micro-receiver comprises a double-clamped meandering titanium suspension along with a mounting platform, two piezoelectric elements attached to the clamped arms of the meandering suspensions, and a laterally magnetized square permanent magnet attached to the center platform (on the side opposite to the piezo-elements). A rectangular coil is attached to the base frame so that it surrounds the magnet. The operation relies on a resonant structure combining both ED and PE transductions. Under the

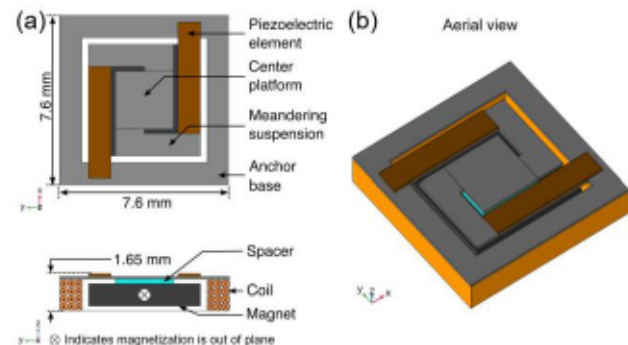


Figure 1: Schematics of the dual-transduction mode wireless power transmission receiver: (a) top and cross-sectional and (b) aerial views.

influence of an external time-varying magnetic field, the structure generates electrical power while oscillating in torsional resonance. A silicon spacer provides clearance between the magnet and the suspension during torsional oscillation. The two piezoelectric elements are connected electrically in series. The coil leads are independent of the piezoelectric leads, so that the system has two simultaneous power generation output ports. The overall dimensions of the micro-receiver are $7.6 \times 7.6 \times 1.65 \text{ mm}^3$. By placing the micro-receiver under a spatially distributed, time varying magnetic field of desired frequency and amplitude, a torsional vibration is produced due to a torque induced on the receiver's magnet. This generates a dynamic stress on the piezoelectric elements which is then converted to electricity by means of the piezoelectric effect. Simultaneously, the motion of the magnet induces an electromotive force (emf) in the receiver coil by means of Faraday's law of induction. In both transduction modes, maximum voltage and power generation are achieved at the torsional resonance of the mechanical suspension and when the receiver is oriented perpendicular to the applied magnetic field.

The resonance behavior of the structure is modeled by a 3D finite-element analysis (FEA) simulation using COMSOL Multiphysics[®]. Figure 2(a) shows the first (torsional) mode of vibration and the corresponding resonant frequency (732.6 Hz). As shown in Figure 2(b), a frequency-domain FEA simulation is carried out to investigate the frequency response for different electrical connections of the transducers, namely: i) PE short-circuit ED open-circuit, ii) both PE and ED open-circuit, iii) PE open-circuit ED short-circuit, and iv) both PE and ED short-circuit. The simulation uses a $50 \mu\text{T}_{\text{rms}}$ field and mechanical damping ratio of $\zeta = 0.006$ (corresponds to measured Q-factor of 82). From the simulation results, it is observed that the impedance of the PE transducer (shorted or open) has an influence on the resonant frequency of the system regardless of whether the ED transducer is open- or short-circuited. The maximum

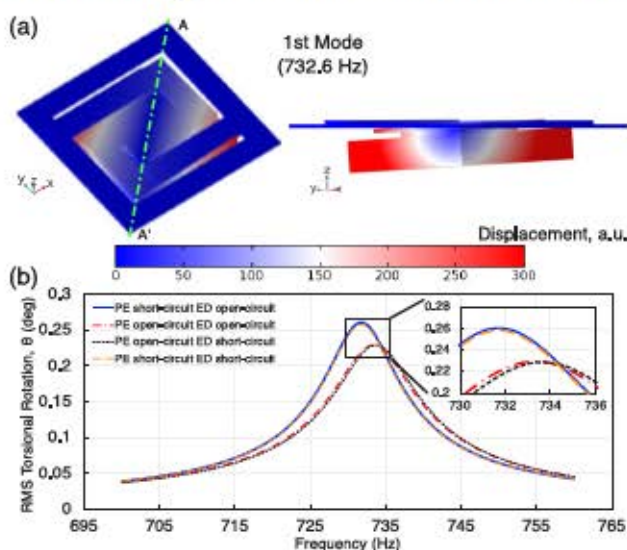


Figure 2: (a) Modal analysis to illustrate torsional (1st mode) resonance and (b) frequency response for torsional rotation angle of the receiver obtained by FEA simulation under $50 \mu\text{T}_{\text{rms}}$ field with $\zeta = 0.006$ ($Q = 82$).

torsional rotation angle of 0.26° is reached when both PE and ED are short-circuited and the corresponding resonant frequency is 731.7 Hz. When both are open-circuited, the maximum torsional rotation angle and the corresponding resonance frequency are 0.23° and 733.3 Hz, respectively. It is evident that the torsional rotation of the magnet is very small which limits the induced emf voltage in the ED transducer. An optimized piezo thickness would increase the rotational angle (by achieving optimal equivalent suspension stiffness) and hence, the voltage/power generated by both PE and ED transducers.

FABRICATION AND ASSEMBLY

Figure 3(a) shows the schematics of the fabrication and assembly process steps. The suspension structure with a center platform and surrounding base was formed by laser micro-machining 125 μm thick titanium (Ti) shim stock. The width of the suspension beam and the area of the center platform were 1 mm and $2.6 \times 2.6 \text{ mm}^2$, respectively. A same-sized ($2.6 \times 2.6 \text{ mm}^2$) silicon (Si) spacer, diced out of a 200- μm -thick Si wafer, and a laterally magnetized N50 NdFeB magnet ($5 \times 5 \times 1 \text{ mm}^3$) were bonded to one side of the center platform using cyanoacrylate. A custom, commercially wound, rectangular, self-supported copper coil (44 AWG, 328 turns, 71Ω resistance) of inner dimension $5.6 \times 5.6 \times 1.4 \text{ mm}^3$ was glued to the surrounding base. On the other side of the suspension, two PZT-5A piezo-patches ($5 \times 1 \times 0.13 \text{ mm}^3$) with sputtered nickel electrodes, poled through the thickness, and diced from a large sheet (Piezo Systems, USA), were bonded to the clamped arms of the suspension beam using electrically conductive silver epoxy (EO-21M-5, Epoxy Set Inc., USA) that forms a series electrical connection between the piezo-patches. Finally, the assembled structure was bonded to a printed circuit board (PCB), and electrical connections were created for measurements. Figure 3(b) shows the photographs of the fully assembled, ready-to-test prototype with its size compared to a US quarter dollar.

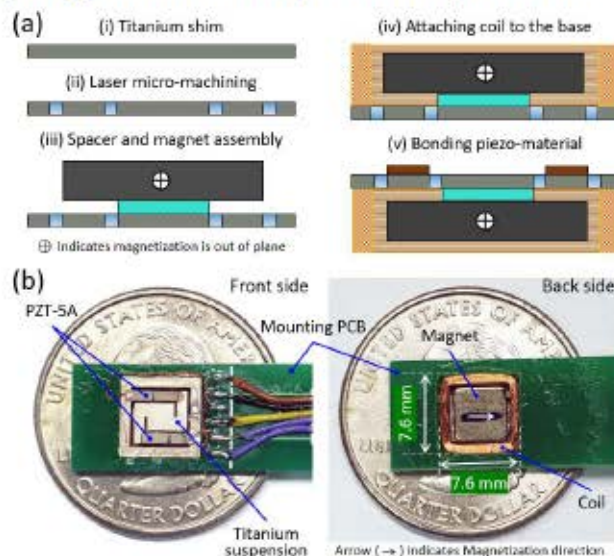


Figure 3: (a) Schematics of the fabrication and assembly process steps of the receiver and (b) photographs of the ready to test, fully assembled prototype with size compared to the US quarter dollar.

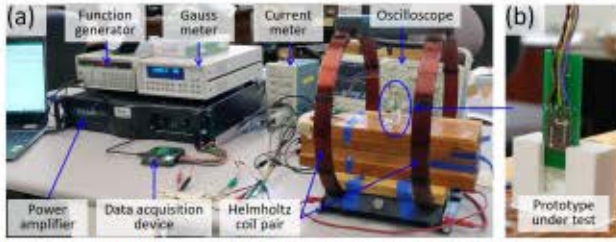


Figure 4: Photographs of (a) the experimental setup and (b) the prototype under test.

RESULTS AND DISCUSSION

First, the ready-to-test micro-receiver was placed at the centroid of a Helmholtz coil pair (28 cm diameter, 15 cm long, 0.74 mT/A), as shown in Figure 4. A voltage signal was generated by an arbitrary waveform generator (Stanford Research Systems DS345) and was fed into a power amplifier (Crown K1) from which the output current was fed into the Helmholtz coil pair. The field strengths were measured using a transverse Hall probe (Lakeshore XHMM-1482) and a gaussmeter (Lakeshore 475DSP). A digital storage oscilloscope (Tektronix DPO-2004 B) was used to measure the input voltage and current to the Helmholtz coil pair, and a USB digital oscilloscope (Diligent Analog Discover 2) was used to measure the output voltage from the prototype.

The open-circuit torsional resonant frequency of the dual-mode micro-receiver was determined by measuring the open-circuit output voltages as a function of frequency as shown in Figure 5. This sweep was performed at a fixed amplitude magnetic field strength ($50 \mu\text{T}_{\text{rms}}$). The output voltages were measured from the series connected PE transducers while the ED transducer was left open-circuited and from the ED transducer while the series PE transducers were kept short-circuited. For each case, the torsional resonant frequencies of the receiver were 732.4 Hz and 730.6 Hz, respectively. As seen from the figure, the micro-receiver exhibits linear characteristics with peaks at resonance that indicates an underdamped 2nd-order system with Q-factor of ~ 82 (in air).

Next, an optimum load sweep was performed on each transducer by connecting a variable load across the output terminals for the cases described earlier (Fig. 5). Each sweep was performed at $50 \mu\text{T}_{\text{rms}}$, and at the resonant frequency of each respective case. The time-average power was calculated using V_{rms}^2/R_L , where V_{rms} was the measured rms voltage across each load resistance R_L . As shown in Figure 6, the series connected PE transducers had an optimum load of 525 k Ω to which a maximum

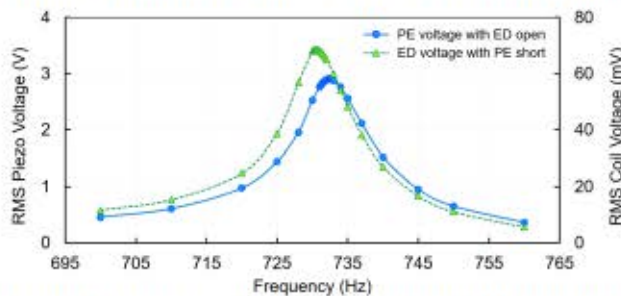


Figure 5: Open-circuit voltage vs. frequency measured from the piezoelectric (PE) and electromagnetic (ED) transducers of the receiver at $50 \mu\text{T}_{\text{rms}}$ magnetic field.

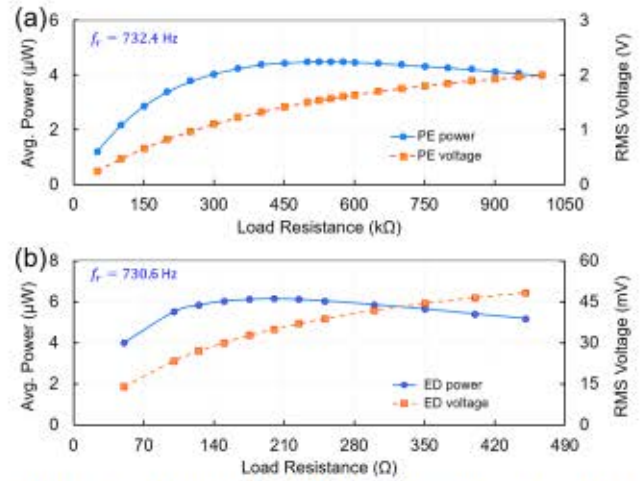


Figure 6: Measured voltage and power vs. load resistance at corresponding resonant frequencies (f_r) of the (a) piezoelectric and (b) electrodynamic transducers of the receiver under $50 \mu\text{T}_{\text{rms}}$ magnetic field.

$4.49 \mu\text{W}$ power was delivered whereas the optimum load for the ED transducer was determined as 200 Ω with a maximum $6.14 \mu\text{W}$ power delivered.

After finding the optimum load for each independent transducer, a frequency sweep was performed to determine the resonant frequency when both transducers were connected to the corresponding optimum load resistances (shown in Fig. 7 inset). With both transducers optimally loaded, the resonant frequency was found to be 734.6 Hz. Note that this frequency was higher than the open-circuit resonant frequency of 732.4 Hz which was unexpected and has yet to be investigated. Next, the time-average power for each transducer was measured as a function of the magnetic field strength, keeping the frequency at 734.6 Hz and the corresponding optimum load connected to each transducer. Low fields (30–120 μT_{rms}) were chosen to determine the onset of nonlinear behavior in the system. As seen in Figure 7, nonlinearity started at field strengths around $70 \mu\text{T}_{\text{rms}}$. This nonlinearity likely occurs due to the mechanical spring stiffening effect at higher field amplitudes.

Lastly, a different coil system was used to measure the power as a function of distance between the transmitter and the micro-receiver. The Helmholtz coil pair was replaced with a single pancake coil (15 cm diameter, 1.5 cm thick, 2.1 mT/A). The micro-receiver was placed on a stationary block and the transmitter coil

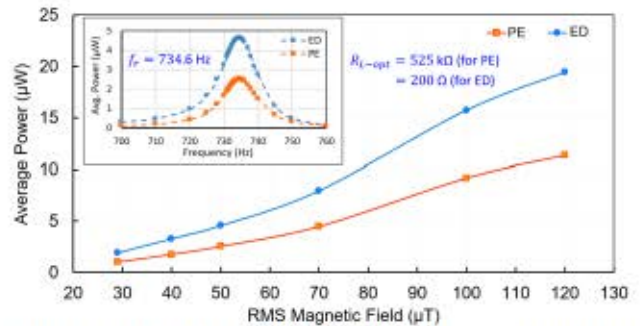


Figure 7: Measured power delivered to corresponding optimum load of the PE and ED transducers of the receiver under various magnetic fields at resonance.

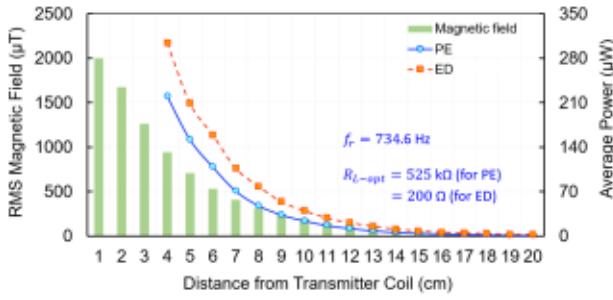


Figure 8: Measured time-average power and magnetic field vs. axial distance at resonance.

was placed on a sliding mount. The transmitter was set to generate a 2 mT_{rms} field (within the human exposure safety limit for 734.6 Hz operating frequency) at an axial distance of 1 cm from its centroid. Starting at 20 cm, the transmitter coil was brought closer to the receiver, and the average power for each transducer was calculated. The field strengths at each respective position were also measured. As shown in Figure 8, the maximum time-average powers simultaneously generated by the PE and ED transducers were 220 μW and 303 μW, respectively when the receiver was placed as close as 4 cm to the transmitter coil, where the field strength was 944 μT_{rms}. Adding these powers together produced a theoretical maximum power of 523 μW. The load voltages for the PE and ED transducers at this condition were 10.75 V_{rms} and 0.25 V_{rms}, respectively. When the transmitter was moved closer than 4 cm, one of the piezo patches cracked, and the device performance dropped substantially; so no more data was collected. Considering the power vs. distance performance, the micro-receiver prototype was still able to generate meaningful power (24 μW by the PE and 39 μW by the ED transducers) at 10 cm distance, where the magnetic field strength was 192 μT_{rms}.

CONCLUSION

In this work, we successfully demonstrated a chip-sized, low-profile dual-transduction mode electrodynamic WPT micro-receiver for low-frequency, near-field wireless power transmission. This micro-receiver generated a maximum power of 523 μW when operated at a 734.6 Hz resonant frequency at an axial distance of 4 cm from a transmitter coil operating within IEEE safety standards for human exposure limit at this frequency (2.8 mT_{rms}). When compared to prior art, this volume-efficient, dual-transduction mode micro-receiver exhibits a significantly improved power density (PD) and normalized power density (NPD), as summarized in Table 1. The NPD was computed at 4 cm (the closest recorded distance to the transmitter coil) and at 10 cm (a practical distance for operation with biomedical implants).

This work successfully blended the two transduction schemes to produce a dual-mode device with the desirable aspects of each mode: an increased NPD, a high voltage output, and a low physical profile. Although the previously reported ED device, [5], has a substantially higher NPD, its main drawback is its large profile and comparatively low voltage output. The dual-mode device compensates for these disadvantages as it has a thickness roughly one-third that of the ED device and a 4.2x higher

Table 1: Summary of performance compared to prior state-of-the-art devices.

Parameter	ED [5]	PE [6]	This work
Volume (cm ³)	0.31	0.08	0.09
Thickness (mm)	4.7	1.5	1.65
Resonance (Hz)	821	724	734.6
*Load Voltage (V _{rms})	2.5	11.5	10.8 (PE) 0.25 (ED)
*Power (mW)	2.48	0.21	0.52
*PD (mW·cm ⁻³)	7.9	2.6	5.8
*NPD (mW·cm ⁻³ ·mT ⁻²)	22.1	5.5	6.5
† NPD (mW·cm ⁻³ ·mT ⁻²)	98.4	11.7	18.1

*At 4 cm and †at 10 cm (from the transmitter coil)

output voltage. Compared to the pure PE device, [6], the dual-mode receiver exhibits a significant increase in NPD. At 4 cm this increase is ~18% but at 10 cm the increase is ~55%. In short, because of its low operational frequency (<1 kHz) and low profile (1.65 mm) design, the dual-transduction mode micro-receiver has great potential use in biomedical implants and wearables.

ACKNOWLEDGEMENTS

This work was supported in part by the NSF I/UCRC on Multi-functional Integrated System Technology (MIST) Center (NSF Grant IIP-1439644, IIP-1439680, and IIP-1738752).

REFERENCES

- [1] J. Huang, Y. Zhou, Z. Ning and H. Gharavi, "Wireless power transfer and energy harvesting: current status and future prospects", *IEEE Wirel. Commun.*, vol. 26, Aug. 2019, pp. 163–169.
- [2] S. R. Khan, S. K. Pavuluri, G. Cummins and M. P. Y. Desmulliez, "Wireless power transfer techniques for implantable medical devices: a review", *Sensors*, vol. 20, Jun. 2020, Art. No. 3487.
- [3] A. Garraud and D. P. Arnold, "Advancements in electrodynamic wireless power transmission", *IEEE Sensors Conference*, Oct. 2016, pp. 82–84.
- [4] IEEE, "Standard for safety levels with respect to human exposure to electric, magnetic, and electromagnetic fields, 0 Hz to 300 GHz", *IEEE Std. C95.1-2019*, Oct. 2019, pp. 1–312.
- [5] M. A. Halim, S. E. Smith, J. M. Samman and D. P. Arnold, "A high-performance electrodynamic micro-receiver for low-frequency wireless power transfer", *IEEE MEMS Conference*, Jan. 2020, pp. 590–593.
- [6] M. A. Halim, A. A. Rendon-Hernandez and D. P. Arnold, "An electrodynamic wireless power receiver 'Chip' for wearables and bio-implants", *IEEE PELS Workshop on Emerging Technologies: Wireless Power*, Nov. 2020.
- [7] M. A. Halim, M. H. Kabir, H. Cho and J. Y. Park, "A frequency up-converted hybrid energy harvester using transverse impact-driven piezoelectric bimorph for human-limb motion", *Micromachines*, vol. 10, Oct. 2019, p. 701.

CONTACT

*D.P. Arnold, tel: +1-352-392-4931; darnold@ufl.edu